Effect of substrate roughness on the magnetic properties of thin fcc Co films

S. J. Steinmuller, C. A. F. Vaz,* V. Ström,† C. Moutafis, D. H. Y. Tse, C. M. Gürtler, M. Kläui,‡ and J. A. C. Bland

Cavendish Laboratory, University of Cambridge, J. J. Thomson Avenue, Cambridge CB3 0HE, United Kingdom

Z. Cui

Rutherford Appleton Laboratory, Chilton, Didcot OX11 0QX, United Kingdom

We present a study of the influence of substrate roughness on the magnetic properties of thin fcc Co films (7 and 17 nm thick) grown on Cu(001)/Si(001). A significant decrease in cubic anisotropy with increasing film roughness was observed with Brillouin light scattering and magneto-optical Kerr effect magnetometry. In addition, the rougher samples showed a substantial broadening of the spin wave peaks. Both effects were found to be more pronounced for the thinner Co layers. Our observations are discussed in the framework of a theoretical model which takes into account the morphology of the Co films as measured by atomic force microscopy. While roughness effects are usually discussed in the context of Néel's "orange-peel" model, we propose a qualitatively different effect in this work whereby the magnetization follows coherently the substrate morphology ("undulating" state) resulting in the absence of magnetic surface charges. This magnetic configuration gives rise to a reduction in the magnetic anisotropy of epitaxial thin films, which is in good qualitative agreement with the experimental observations.

PACS number(s): 75.30.Gw, 75.70.−i, 75.30.Ds, 68.55.Jk

I. INTRODUCTION

Roughness at surfaces and interfaces has crucial implications for the physics of thin films and multilayer systems, and several methods and experimental techniques have been developed to provide a good microscopic characterization of the surface morphology, such as x-ray scattering and atomic force microscopy (AFM). Magnetic systems, in particular, have been shown to be very sensitive to the surface morphology and roughness, the latter affecting the magnetic *M-H* characteristic,[1–3] the magnetization switching mechanism,[4] and the effective magnetic coupling in multilayer systems[5] through the so-called orange-peel effect.[6] The latter effect is of special importance in the context of giant magnetoresistance and tunnel magnetoresistance multilayer structures.[7–10]

In Néel's orange-peel model, the effect of surface roughness is that of creating a surface magnetic charge distribution that contributes an extra term to the magnetic energy. This additional magnetostatic energy term leads to a reduction in the perpendicular uniaxial surface magnetic anisotropy,[11–13] but otherwise is isotropic in the plane of the film. A different magnetic configuration may be envisaged in ultrathin films when the magnetization distribution follows coherently the substrate morphology. In this case, volume instead of surface charges are generated, in direct contrast to the orange-peel effect; adapting Néel's analogy for the configuration we propose, one could speak of an "apple-peel" effect, where the magnetization follows smoothly the surface profile of the substrate. For ultrathin epitaxial magnetic films, this mechanism will result in an extra contribution to the magnetic anisotropy.[14]

For our experimental studies of the effect of roughness on the magnetic properties of thin epitaxial films, we chose to investigate fcc Co layers grown on Cu(001)/Si(001). This is a well studied and characterized system,[15–17] allowing us to directly relate any observed changes in magnetic behavior to the morphology of the film. By modeling the roughness contribution to the effective magnetocrystalline anisotropy constants, we are able to explain the observed decrease in anisotropy. Our model furthermore enables us to quantify the contribution of film roughness to the magnetic anisotropy as a function of the roughness parameters of the epitaxial magnetic film.

II. SAMPLE GROWTH AND SURFACE MORPHOLOGY

For the present study, two sets of epitaxial fcc Co samples were prepared with different nominal film roughnesses. The Co films were deposited onto 100 nm thick Cu(001) buffer layers grown on undoped Si(001) substrates with different surface treatments: a smooth surface was obtained after removal of the native oxide layer of a polished Si wafer upon etching in a 10% HF solution for 10 min prior to the sample growth; a rougher Si substrate was obtained by reactive ion etching the Si substrate using SF_6+O_2 for 1.5 min, after which it was etched in a 10% HF solution for removal of native oxides prior to the metal growth. The metal layers were deposited in an ultrahigh vacuum molecular beam epitaxy chamber, with a base pressure of $\sim 3 \times 10^{-10}$ mbar. The layer thickness was monitored by a calibrated quartz microbalance. A 100 nm thick Cu(001) layer was deposited on the Si substrate, which develops an ordered (001) surface rotated by 45° with respect to the Si lattice, suitable for epitaxial growth of the fcc Co phase, which grows in registry with the Cu(001) surface;[16,17] two Co thicknesses were studied, 7 and 17 nm. A 4 nm thick Cu layer was deposited onto the Co layers so that a similar interface is present at the top and bottom, and the structure was finally capped with 3 nm Au in order to prevent oxidation during the *ex situ* measurements.
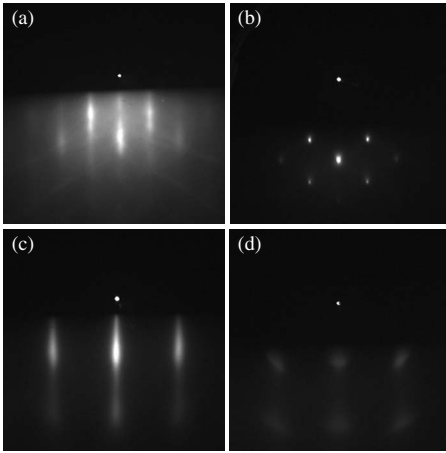
FIG. 1. RHEED images along the [110] Si(001) azimuth of the (a) smooth and (b) rough Si(001) substrate, as well as the (c) smooth and (d) rough 7 nm Co layer.

In Fig. 1, we show reflection high energy electron diffraction (RHEED) images of the Si(001) substrate and the Co layer for the rough and smooth samples; it is observed that while the smooth Si substrate presents streaky diffraction spots and Kikuchi lines [Fig. 1(a)] characteristic of smooth surfaces, the rough Si substrate shows a diffraction pattern [Fig. 1(b)] typical of rough substrates with large asperities, corresponding, in fact, to a transmission diffraction pattern. The RHEED patterns of the Co layers [Figs. 1(c) and 1(d)] also show that the film grown on the rougher Si substrate displays much broader diffraction spots, indicative of a much rougher Co film.

This qualitative assessment of the surface morphology was confirmed and quantified by AFM and scanning electron microscopy (SEM) measurements. Characteristic AFM images of the 7 nm thick Co samples are shown in Fig. 2, revealing a significant difference in the degree of film roughness. Values for the roughness correlation length ξ and amplitude σ of all the investigated samples extracted by fitting the autocorrelation function determined from the measured AFM data are given in Table I. While ξ is found to be almost identical for the four Co films, σ is larger by a factor of 10 for the rough samples. Similar results were obtained by SEM (not shown).[18] For the rough samples, σ is of the same order of magnitude as the Co film thickness. Furthermore, the roughness parameter $4\sigma/\xi$ (i.e., the average "slope" of the film roughness) is relatively large for both rough Co samples (0.28±0.03 for the 7 nm and 0.28±0.02 for the 17 nm Co samples). If we assume that the undulation of the Co layer follows the surface morphology of the bottom Cu layer (i.e., both Co/Cu interfaces are coherent), which ought to be the case since Co tends to grow in a layer by layer mode on Cu(001) surfaces,[15] a cross-section profile as depicted in the inset of Fig. 7 would be expected. This picture is further supported by the fact that $4\sigma/\xi$ is, within errors, identical for both Co thicknesses, i.e., no smoothening of the films is observed when more material is deposited. In order to further investigate the detailed sample structure, we performed cross-sectional transmission electron microscopy (TEM) measurements on the rough 17 nm Co sample. A character-
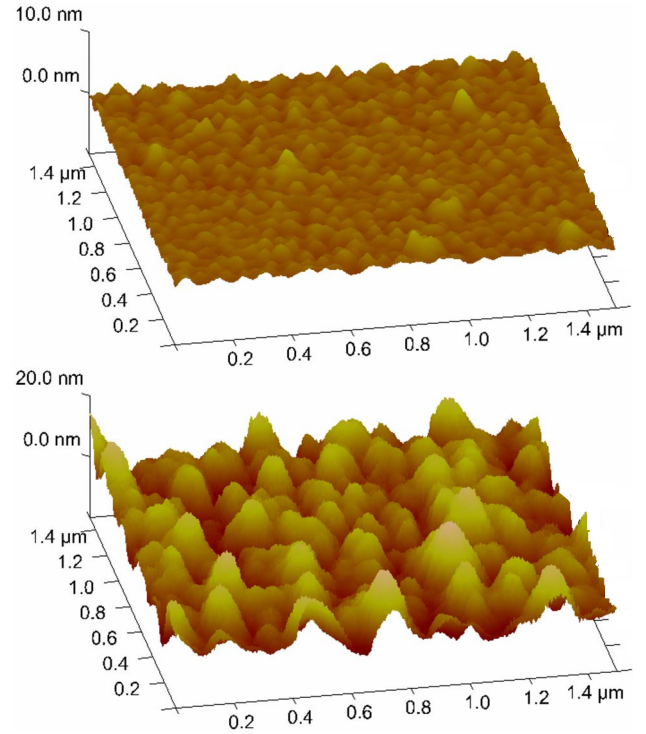

FIG. 2. (Color online) AFM images of the smooth (top) and the rough (bottom) 7 nm Co sample.

istic TEM image is shown in Fig. 3. While the Cu and Co layers cannot be distinguished in our experiments (due to their similar transparencies for the electron beam energy used, 200 keV), the Au film can be clearly identified. It grows in registry with the underlying Cu surface and exhibits a relatively uniform thickness in the whole sample area probed. The details of the surface morphology (ξ and σ) are in reasonable agreement with the AFM results (see Table I). However, it has to be noted that the Si/Cu interface and the Cu/Au interface do not seem to be coherent. A possible explanation for this observation may be interdiffusion at the Si/Cu interface, resulting in the formation of a Cu silicide layer possibly enhanced due to the TEM sample preparation procedure. This would also account for the fact that the total thickness of the metal structure measured with TEM ($\sim$170 nm) is larger than its nominal thickness (124 nm). It is apparent that our TEM data do not allow for definite conclusions on the exact morphology or thickness uniformity of the Co layer. However, taking into account the corrugation at the Cu/Au interface (Fig. 3), which is in close proximity (4 nm) to the relatively thin Co layer, it is safe to assume that the Co film exhibits a significant degree of undulation. Nevertheless, a decrease in thickness uniformity for the rougher films cannot be ruled out completely.

III. MAGNETIC CHARACTERIZATION

The influence of film roughness on the magnetic properties of thin fcc Co films grown on Cu(001)/Si(001) was investigated by means of Brillouin light scattering (BLS), superconducting quantum interference device (SQUID)

TABLE I. Roughness correlation length ξ, roughness amplitude σ, saturation magnetization M_s, cubic anisotropy constants K_1, and coercive fields H_C of the investigated Co samples, determined by AFM (ξ, σ), BLS (M_{BLS}, K_{1BLS}), SQUID (M_{SQUID}), and MOKE (K_{1MOKE}, H_C), respectively; literature values for bulk Co and two thin Co films (6.5 and 10 nm) grown on Cu/Si are also given for comparison.

	ξ (nm)	σ (nm)	M_{BLS} (10^3 emu/cm^3)	M_{SQUID} (10^3 emu/cm^3)	K_{1BLS} (10^3 erg/cm^3)	K_{1MOKE} (10^3 erg/cm^3)	H_C (Oe)
Smooth Co (7 nm)	50±20	0.43±0.07	1.7±0.1	1.2±0.3	−6.4±0.1	−12±4	92±11
Rough Co (7 nm)	65±5	4.53±0.07	1.7±0.1	1.5±0.3	−4.8±0.2	−8.0±3.0	123±8
Smooth Co (17 nm)	55±5	0.54±0.07	1.5±0.2	1.2±0.3	−5.1±0.3	−8.4±3.0	63±11
Rough Co (17 nm)	93±5	6.42±0.08	1.5±0.2	1.6±0.3	−4.7±0.3	−6.5±2.5	84±11
Bulk Co			1.4 1[a]		−12 2[b]		
Co (6.5 nm)					−6.1[c]		
Co (10 nm)					−4.6[d]		

[a]References 19 and 20.
[b]Reference 21.
[c]Reference 22.
[d]Reference 16.

magnetometry, and longitudinal magneto-optical Kerr effect (MOKE) magnetometry. All measurements were carried out at room temperature.

In the BLS experiment, the frequency shift of light inelastically scattered from magnons is measured, allowing for the identification of the spin wave frequencies in a given system. The measurements reported here were performed in the backscattering geometry with the plane of incidence orthogonal to the applied field. An Ar$^+$-ion laser with a wavelength of 514.5 nm was used at an angle $\theta = 45°$ with respect to the sample plane normal, corresponding to a probed spin wave number of 1.73×10^7 m^{-1}. By varying the experimental conditions, such as the applied magnetic field strength and direction, a number of magnetic parameters (e.g., magnetization, anisotropies, and g-factor) can be determined with a high degree of accuracy. Due to the reduced thicknesses of the Co layers, only Damon-Eshbach (DE) surface spin wave modes[23] are observed in the investigated frequency range. In the first set of experiments, the applied in-plane field was kept constant at 1 kOe (which is sufficient to saturate the Co films in plane, see M-H curves in Fig. 6) and the angle η between the magnetic field and the magnetic hard axis (crystallographic [100] direction) was varied from −90° to +90°.
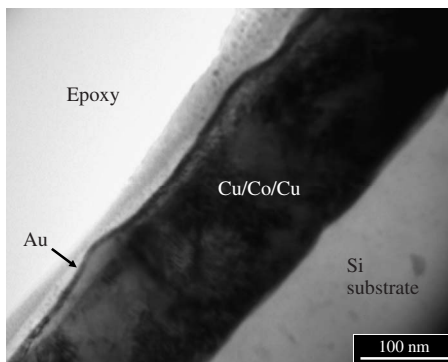
The angular dependence of the spin wave frequency ν is shown in Fig. 4 for the 7 nm thick Co samples. For both the smooth and the rough sample, ν shows a periodic dependence on η with a periodicity of 90°, reflecting the in-plane cubic anisotropy of the Co films.[16,22] As is apparent, this oscillation has a smaller amplitude for the rougher Co layer. The same behavior was observed for the 17 nm thick films, however, with a less pronounced difference between the two samples. In a second set of experiments, the magnetic field was applied at a constant angle $\eta = 45°$ (i.e., along the crystallographic [110] direction) and varied from 1 to 9 kOe (not shown). The variation of the DE mode frequency with external field amplitude and direction allows for the saturation magnetization M_s, the g-factor, and the anisotropy constants to be determined. In order to obtain these parameters, we iteratively fitted our measured data using the continuum model proposed by Rado and Hicken,[24] which takes into account both dipolar and exchange interactions. It is impor-

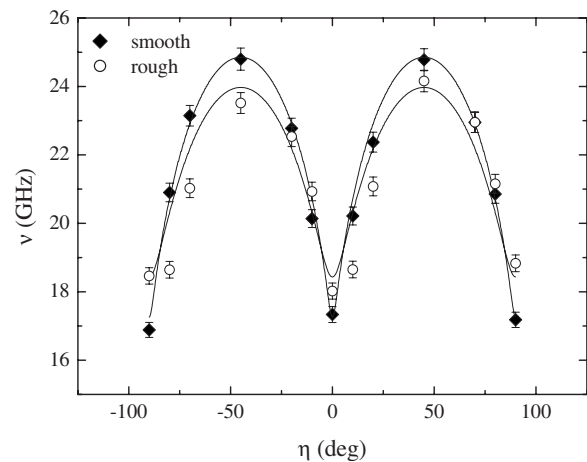FIG. 3. Cross-sectional TEM image of the rough 17 nm Co sample.

FIG. 4. Spin wave frequency vs applied magnetic field angle ($H = 1$ kOe) for the smooth (solid diamonds) and the rough (empty circles) 7 nm Co sample. The solid lines are fits to the data based on the theoretical model described in Ref. 24.
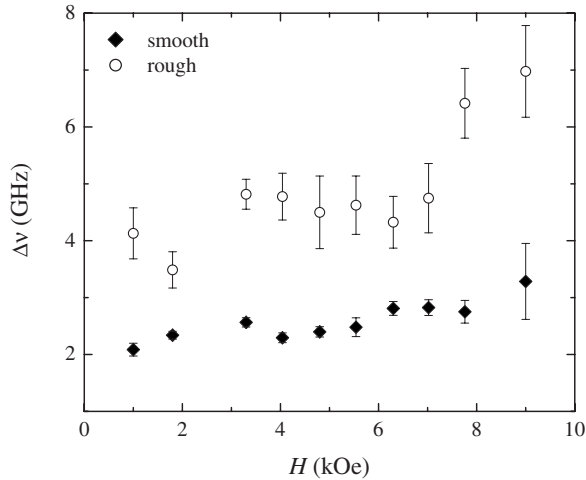
FIG. 5. Spin wave peak linewidth vs applied magnetic field amplitude ($\eta = 45°$) for the smooth (solid diamonds) and the rough (empty circles) 7 nm Co sample.
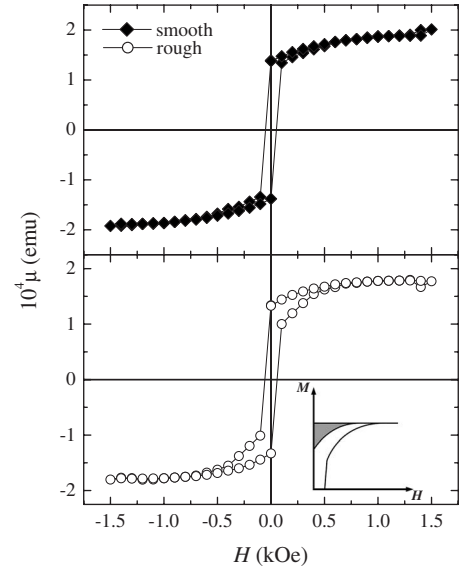

FIG. 6. *M-H* characteristics measured along the hard magnetic axis by SQUID for the smooth (solid diamonds) and the rough (empty circles) 7 nm Co sample. In the inset, a schematic of a hysteresis loop is shown with the gray filled area denoting the demagnetizing energy.

tant to note that since M_s has an influence on both the angular and the field dependence of ν, both sets of data were fitted simultaneously. Angular fits for the 7 nm thick Co films are shown in Fig. 4 (solid lines). The *g*-factor was found to be 2.21 ± 0.05 for all investigated samples, which is close to the value reported for a 105 nm thick fcc Co(100) film by Liu *et al.*[25] ($g = 2.08 \pm 0.02$). No measurable in-plane uniaxial anisotropy was observed, in agreement with earlier ferromagnetic resonance studies on similar structures.[16] Table I shows values for M_s and the cubic anisotropy constant K_1 obtained from the BLS measurements. In this paper, the following definition of K_1 is used:

$$e_{ani} = K_1(\alpha_1^2 \alpha_2^2 + \alpha_2^2 \alpha_3^2 + \alpha_3^2 \alpha_1^2), \quad (1)$$

where e_{ani} is the anisotropy energy density and α_i are the direction cosines of the magnetization. We find no influence of the surface morphology on the sample magnetization, and the values determined for M_s agree reasonably well with that of bulk fcc Co.[19,20] $|K_1|$ was found to decrease with increasing thickness, as observed for fcc Co in this thickness range.[16,22] In addition, a significant reduction in cubic anisotropy was observed for the rough samples that is more pronounced for the thinner pair of Co films. The origin of this effect will be discussed in detail in the following section.

Furthermore, the spin wave peaks measured with BLS were found to be considerably broader for the rougher films over the whole angular and field ranges. Figure 5 shows a comparison of the full width at half maximum peak linewidths $\Delta\nu$ for the two 7 nm Co samples as a function of the applied magnetic field. The thicker pair of samples shows the same behavior but, as for the DE mode frequency shift discussed above, the differences are less pronounced. For ultrathin magnetic films, the observation of remarkably broad spin wave peaks has been reported by Kerkmann *et al.*[26] They observed a spin wave peak linewidth of the order of 10 GHz for 1 ML (monolayer) of Co grown on Cu(100). Stamps *et al.*[27] attributed this effect to the influence of imperfections and surface roughness. In their simplified theo-

retical approach (exchange interaction was not included), they investigated two mechanisms: scattering of spin waves by imperfections (such as "bumps" or holes on the surface) into different states and formation of new allowed spin wave modes due to changes in the local anisotropy field caused by thickness variations. The first effect is found to be relatively small and cannot explain the increase in linewidth observed for our rough set of samples. The second mechanism relies on the assumption that the film roughness induces local changes in film thickness, which is not expected to be the case for our magnetic layers. As detailed above, the Co films should closely follow the surface morphology of the Cu(001)/Si(001) substrates and consequently have a homogeneous thickness within the probed area. In the following section, we will introduce a third spin wave peak broadening mechanism which we believe to be responsible for the effects observed in our measurements.

In order to gain further information about the magnetic sample properties and to confirm the results obtained by BLS, SQUID and longitudinal MOKE measurements were carried out. Hysteresis loops for the Co (7 nm) samples measured along the hard magnetic axis by SQUID are shown in Fig. 6. Both curves show a very similar field dependence and exhibit the shape characteristic for a cubic hard axis. Close to the coercive field H_C, however, a steplike feature is observed that is much more pronounced for the rough samples (Fig. 6, bottom) and disappears when the field is applied along the easy magnetic axis. This finding will be discussed in the following section. The SQUID data allow us to estimate M_s for comparison with the BLS results (see Table I), and the resulting values are found to be in good agreement. The relatively large errors are mainly due to inaccuracies in the determination of the sample volume. Both SQUID and MOKE measurements revealed an increase in coercive field H_C for

the rougher samples, as has been observed in previous studies.[1–3] Values for H_C measured by MOKE with the magnetic field applied along the easy magnetic axis are shown in Table I. Furthermore, an angular dependent MOKE study enabled us to determine K_1, allowing for a comparison with the results obtained by BLS. The angle between the easy magnetic axis and the applied field was varied from 0° to 180° in steps of 5° and hysteresis loops were recorded. The demagnetizing energy, which approximately equals the anisotropy energy,[28] was then calculated for each corresponding angle (see inset of Fig. 6). Finally, plotting e_{ani} versus the applied magnetic field angle η and fitting the resulting curve to the anisotropy energy density expression for a thin fcc Co(001) film,

$$e_{ani} = (K_1/4)\sin^2(2\eta), \qquad (2)$$

allowed us to obtain the cubic anisotropy constant K_1. Since the measured Kerr intensity cannot give the sample magnetic moment, the MOKE curves were normalized and the saturation magnetization values obtained by BLS were used. The resulting values for K_1 are shown in Table I. This method for determining the anisotropy constants (which is described in detail, for example, in Ref. 28) is less accurate than the angular dependent BLS measurements discussed above, which is reflected by the relatively large errors found for K_{1MOKE}. It is, however, a reliable way of determining relative changes in anisotropy. As can be seen, K_{1MOKE} is in reasonable agreement with K_{1BLS} for all four investigated samples. More importantly, a decrease in K_{1MOKE} is observed for the rougher films for both Co thicknesses, which is in good agreement with the BLS experiments.

IV. DISCUSSION

From the previous results, it follows that film roughness is responsible for a decrease in the effective anisotropy of the fcc Co films, and we proceed now to discuss the mechanisms that may be responsible for the observed changes in K_1.

A well-known mechanism which generally contributes to a change in the magnetic anisotropy of epitaxial films is the effect of strain relaxation introduced by roughness;[29] this leads to a decrease in the magnetoelastic energy and therefore to a change in the magnetic energy. In this case, for islands of a given material with a high symmetry plane such as (001), the strain is biaxial, and strain relaxation induced by film roughness leads to a change in the magnetic anisotropy via magnetoelastic interaction.[30] However, for ultrathin films deposited onto a substrate with a given roughness profile as we have been considering in the present work, strain relaxation due to the substrate roughness is less likely (since the thin film grows in registry), although strain relief due to the onset of misfit dislocations could, in principle, modify the in-plane magnetic anisotropy. As mentioned, given the length scale of the Cu(001) substrate roughness, we expect strain relaxation through misfit dislocations to be the dominant mechanism, with a small contribution to the magnetic anisotropy in our thin Co films. Furthermore, K_1 might be affected by the crystal dispersion (mosaicity) present in our samples.[31] However, since the degree of mosaicity is ex-
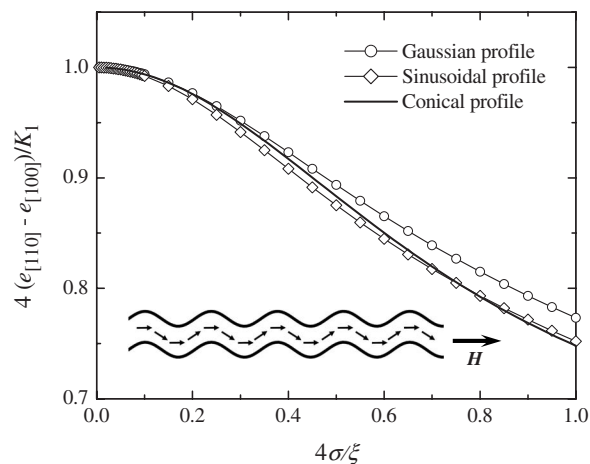

FIG. 7. Normalized anisotropy energy density difference vs roughness parameter $4\sigma/\xi$ for several film roughness shapes. In the inset, a schematic of a rough Co film cross section is shown. The arrows denote the direction of the sample magnetization.

pected to be the same for all four investigated Co layers, this mechanism cannot account for the observed differences in magnetic anisotropy. Interface effects could also play a role in the observed variations of the magnetic anisotropy with roughness (via changes in interface anisotropies,[11] interdiffusion, or changes in the interface magnetic moment), but such effects should be relatively small for 7 and 17 nm thick films where the interface is already a comparatively small portion of the system.

Depending on the values of σ, ξ, and the nominal film thickness d, the sample magnetization **M** could adopt a variety of different configurations: $\sigma \ll d$ would favor an in-plane alignment of **M** along the easy magnetic axis, i.e., the classical uniform state (orange-peel effect), thus minimizing the anisotropy and the exchange energy. There is, however, a magnetostatic contribution to the total magnetic energy due to the presence of magnetic surface (but not volume) charges. On the other hand, for $\sigma \gtrsim d$, **M** should follow the profile of the magnetic layer (inset of Fig. 7), thereby avoiding the creation of surface pole charges. This configuration, which we term the "undulating" state, gives rise to the formation of volume charges and is therefore the exact counterpart of Néel's case. In the general case, the orientation of **M** will be determined by the competition between the different energy contributions (magnetostatic, exchange, and anisotropy), leading to a state which would resemble a mixture of these two extreme cases.

The orange-peel effect is not expected to lead to a change in the in-plane magnetic anisotropy, since for a random surface morphology, all directions in the plane of the film should be equivalent, i.e., the orange-peel effect should be isotropic in the film plane. Since no directional preference in the island orientation is observed in our surfaces, we can rule out this contribution to the magnetic energy as responsible for affecting the in-plane magnetic anisotropy. However, for epitaxial films, the undulating configuration will cause a change in the effective magnetic anisotropy, since there is a change in magnetic energy which is different when the magnetization points along the hard and easy magnetization axes.
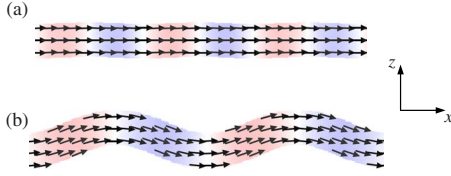
FIG. 8. (Color online) Cross-section magnetization profiles at zero applied magnetic field for the (a) smooth and the (b) rough 17 nm Co sample as simulated by OOMMF. The x axis is along an easy magnetic axis of the system and the z axis is along the surface plane normal. The color scale denotes the z component of **M** and is increased by a factor of 10 for the smooth film in order to facilitate visualization.

We have developed a simple model that aims to estimate the magnitude of this contribution to the magnetic anisotropy.[14] The model consists in calculating the change in the effective magnetic anisotropy for a thin epitaxial film covering a non-magnetic island of a given shape. It assumes that the magnetization follows the film profile in order to avoid the creation of surface pole charges. For simplicity, we considered islands with cylindrical symmetry (namely, with conical, sinusoidal, and Gaussian radial cross sections), and we show that the values obtained do not depend significantly on the shape chosen. This finding gives us confidence that the results of the calculations may have practical relevance. In this model, the changes in anisotropy ensue from the tilting of the magnetization away from the in-plane hard and/or easy axis, leading to a variation of the anisotropy energy contribution and from the fact that this contribution is different for the easy and hard magnetic axes. Simply speaking, for the case of fcc Co(001), the hard axis becomes less hard and the easy axis becomes less easy, resulting in a reduction of the effective magnetic anisotropy. A detailed discussion of this model, including its limitations, is provided in Ref. 14. In Fig. 7, we show the results of our model for the change in the cubic magnetic anisotropy constant as a function of the dimensionless roughness parameter $4\sigma/\xi$, which corresponds to a measure of the island slope. We see that for small values of $4\sigma/\xi$, the change in the anisotropy constant is relatively small, but it increases for larger values of $4\sigma/\xi$. For the $4\sigma/\xi$ values measured for our samples (~ 0.03 for the smooth and ~ 0.3 for the rough samples), we expect a change in K_1 of 0.1% for the smooth films and 4.4% for the rough films in the undulating state.

In order to get an indication of the expected magnetization alignments for the samples investigated in the present study, we performed two-dimensional micromagnetic simulations of a cross section of the Co film using the OOMMF package,[32] assuming bulk fcc Co parameters ($M_s = 1.4 \times 10^3$ emu/cm^3, $K_1 = -1.2 \times 10^6$ erg/cm^3, and exchange constant $A = 3 \times 10^{-6}$ erg/cm). The cell size was $(0.5 \text{ nm})^2$ and the modulation values used were the ones determined by AFM (see Table I). While this is not a simulation of the real three-dimensional film, it reflects the basic features of our system and provides a qualitative description of the mechanisms underlying our picture. The results for the 17 nm Co samples are shown in Fig. 8. It is found that for the rough sample, **M** follows closely the morphology of the Co layer,

TABLE II. Relative changes in magnetic anisotropy as determined experimentally by BLS (ΔK_1^{exp}) and as calculated using our suggested model ($\Delta K_1^{\text{theory}}$) (Ref. 14).

Thickness (nm)	ΔK_1^{exp} (%)	$\Delta K_1^{\text{theory}}$ (%)
7	25±4	4.3
17	8±11	4.3

suggesting that the film is in the undulating state. For the smooth sample, however, only a very small tilt of **M** away from the easy axis direction is observed [it has to be noted that the color scale is increased by a factor of 10 in Fig. 8(a)] and the magnetic configuration is very close to that of the uniform state. The same behavior is observed for the 7 nm Co samples. Similar results have recently been reported for the case of patterned zigzag structures.[33]

We calculated the relative change in anisotropy constant ΔK_1, defined as

$$\Delta K_1 = (K_1^{\text{smooth}} - K_1^{\text{rough}})/K_1^{\text{smooth}}, \qquad (3)$$

for both the values of K_1 given by our model and those obtained experimentally by BLS (see Table II). A comparison of ΔK_1^{exp} with $\Delta K_1^{\text{theory}}$ shows that, while the simplicity of the model does not allow for a very accurate determination of the changes in the measured effective anisotropy, it is sufficient to account for the sign and magnitude of such changes. The observed discrepancy between experiment and theory is likely to be due to the fact that real surfaces tend to be more complex, often with complicated island distributions[34,35] (see Fig. 2, bottom). In addition, the possibility that some degree of smoothening (or roughening) occurs during the growth of the Co films, leading to a nonuniform thickness distribution, cannot be completely excluded in our experiments. Such deviations from a perfect undulating film (as assumed in our model) would influence the extent to which **M** is tilted out of plane and thus affect the measured value of ΔK_1.

Furthermore, our calculations show that if the sample is in the undulating state, ΔK_1 depends only on the roughness parameter $4\sigma/\xi$ but not on the thickness of the magnetic layer. However, experimentally, we observe a significant decrease in ΔK_1 when d is increased from 7 to 17 nm (Table II). This finding might be due to a gradual transition from the undulating to the orange-peel state with increasing Co thickness. While the micromagnetic simulations (which only give a qualitative measure of the magnetization configuration in real surfaces) suggest that for both the 7 and the 17 nm rough Co sample **M** closely follows the roughness of the magnetic layer [Fig. 8(b)], in reality, the tilt of **M** away from the easy axis might be less pronounced for the thicker film. In order to gain more information on the details of the undulating state (e.g., how closely the magnetization follows the film morphology for a given thickness and set of roughness parameters), the magnetization configuration would have to be probed directly. In principle, this could be achievable by off-specular polarized neutron scattering

experiments[36] or x-ray resonant magnetic scattering measurements.[37]

Furthermore, the model detailed above offers a possible explanation for the observed increase in spin wave peak linewidth with film roughness. Since the diameter of the BLS laser spot (~ 500 μm) is significantly larger than the roughness correlation length ξ (Table I), the areas probed in our experiments comprise a large number of Co film undulations. The tilting of the spins away from the easy axis will lead to local variations in the magnetic anisotropy energy, giving rise to new allowed spin wave modes. This interpretation is similar to the explanations given by Stamps *et al.*,[27] with the only difference that in their case the anisotropy field changes are assumed to be induced by film thickness variations. While they restrict their study to ultrathin ($1-3$ ML) films, their main arguments are still applicable to the Co layers investigated in the present work.

The observation of a pronounced steplike feature in the $M-H$ loops of the Co rough samples also lends support to our interpretation. It has been shown for the case of thin epitaxial Fe films grown on GaAs(001) that this behavior can be explained by the persistence of a domain structure up to large magnetic fields (similar to ripple domains) and to the presence of submicrometer scale irregularities in the film structure.[38] For our rough films, the dispersion in the magnetization direction away from the hard axis due to roughness is expected to lead to an increase in hysteresis at fields above the coercive field.

V. CONCLUSIONS

In conclusion, we investigated the effect of film roughness on the magnetic properties of thin fcc Co(001) films. The sample morphology was found to have a strong influence on the cubic magnetic anisotropy: BLS and MOKE measurements revealed a significant decrease in K_1 for the rougher set of samples. Furthermore, the spin wave peak linewidth was found to increase substantially with increasing roughness. Both effects were more pronounced for the thinner pair of samples and could not be understood in the framework of current theory. In order to explain the observed behavior, we introduced a simple model that assumes a magnetic configuration where the sample magnetization closely follows the Co film morphology, the so-called undulating state. Our calculated changes in K_1 are in relatively good agreement with those observed experimentally. Further support to our interpretations is added by micromagnetic simulations that show a substantial effect of the film undulations on the magnetization orientation.

ACKNOWLEDGMENTS

*Present address: Applied Physics, Yale University, New Haven, Connecticut 06520, USA.

†Present address: Department of Materials Science and Engineering, Royal Institute of Technology, SE-100 44 Stockholm, Sweden.

‡Present address: Fachbereich Physik, Universität Konstanz, 78457 Konstanz, Germany.

[1] Q. Jiang, H.-N. Yang, and G.-C. Wang, Surf. Sci. **373**, 181 (1997).

[2] M. Li, Y.-P. Zhao, G.-C. Wang, and H.-G. Min, J. Appl. Phys. **83**, 6287 (1998).

[3] M. Li, G.-C. Wang, and H.-G. Min, J. Appl. Phys. **83**, 5313 (1998).

[4] P. Rosenbusch, J. Lee, G. Lauhoff, and J. A. C. Bland, J. Magn. Magn. Mater. **172**, 19 (1997).

[5] L. Néel, Compt. Rend. **255**, 1676 (1962).

[6] L. Néel, Compt. Rend. **255**, 1545 (1962).

[7] B. D. Schrag *et al.*, Appl. Phys. Lett. **77**, 2373 (2000).

[8] H. D. Chopra, D. X. Yang, P. J. Chen, D. C. Parks, and W. F. Egelhoff, Jr., Phys. Rev. B **61**, 9642 (2000).

[9] C. Tiusan, M. Hehn, and K. Ounadjela, Eur. Phys. J. B **26**, 431 (2002).

[10] W. F. Egelhoff, Jr., R. D. McMichael, C. L. Dennis, M. D. Stiles, A. J. Shapiro, B. B. Maranville, and C. J. Powell, Appl. Phys. Lett. **88**, 162508 (2006).

[11] P. Bruno, J. Phys. F: Met. Phys. **18**, 1291 (1988).

[12] P. Bruno, J. Appl. Phys. **64**, 3153 (1988).

[13] P. Bruno, G. Bayreuther, P. Beauvillain, C. Chappert, G. Lugert, D. Renard, J. P. Renard, and J. Seiden, J. Appl. Phys. **68**, 5759 (1990).

[14] C. A. F. Vaz, S. J. Steinmuller, and J. A. C. Bland, Phys. Rev. B **75**, 132402 (2007).

[15] B. Heinrich, J. F. Cochran, M. Kowalewski, J. Kirschner, Z. Celinski, A. S. Arrott, and K. Myrtle, Phys. Rev. B **44**, 9348 (1991).

[16] R. Naik, C. Kota, J. S. Payson, and G. L. Dunifer, Phys. Rev. B **48**, 1008 (1993).

[17] B. G. Demczyk, V. M. Naik, A. Lukaszew, R. Naik, and G. W. Auner, J. Appl. Phys. **80**, 5035 (1996).

[18] S. J. Steinmuller, C. A. F. Vaz, V. Ström, C. Moutafis, C. M. Gürtler, M. Kläui, J. A. C. Bland, and Z. Cui, J. Appl. Phys. **101**, 09D113 (2007).

[19] H. P. Myers and W. Sucksmith, Proc. R. Soc. London, Ser. A **207**, 427 (1951).

[20] J. Crangle, Philos. Mag. **46**, 499 (1955).

[21] H. Fujiwara, H. Kadomatsu, and T. Tokunaga, J. Magn. Magn. Mater. **31-34**, 809 (1983).

[22] W. Weber, A. Bischof, R. Allenspach, C. H. Back, J. Fassbender, U. May, B. Schirmer, R. M. Jungblut, G. Güntherodt, and B. Hillebrands, Phys. Rev. B **54**, 4075 (1996).

[23] R. W. Damon and J. R. Eshbach, J. Phys. Chem. Solids **19**, 308 (1961).

[24] G. T. Rado and R. J. Hicken, J. Appl. Phys. **63**, 3885 (1988).

[25] X. Liu, M. M. Steiner, R. Sooryakumar, G. A. Prinz, R. F. C.

Farrow, and G. Harp, Phys. Rev. B **53**, 12166 (1996).

[26] D. Kerkmann, J. A. Wolf, D. Pescia, T. Woike, and P. Grünberg, Solid State Commun. **72**, 963 (1989).

[27] R. L. Stamps, R. E. Camley, B. Hillebrands, and G. Güntherodt, Phys. Rev. B **47**, 5072 (1993).

[28] B. D. Cullity, *Introduction to Magnetic Materials* (Addison-Wesley, Menlo Park, CA, 1972).

[29] J. Y. Tsao, *Materials Fundamentals of Molecular Beam Epitaxy* (Academic, New York, 1993).

[30] C. A. F. Vaz and J. A. C. Bland, J. Appl. Phys. **89**, 7374 (2001).

[31] C. A. F. Vaz, S. J. Steinmuller, C. Moutafis, J. A. C. Bland, and A. Yu. Babkevich, Surf. Sci. **601**, 1377 (2007).

[32] http://math.nist.gov/oommf

[33] W. C. Uhlig and J. Unguris, J. Appl. Phys. **99**, 08G302 (2006).

[34] J. M. Bennett and L. Mattson, *Introduction to Surface Roughness and Scattering* (Optical Society of America, Washington, D.C., 1999).

[35] C. A. F. Vaz, G. Lauhoff, J. A. C. Bland, S. Langridge, D. G. Bucknall, J. Penfold, J. Clarke, S. K. Halder, and B. K. Tanner, J. Magn. Magn. Mater. **313**, 89 (2007).

[36] S. Langridge, J. Schmalian, C. H. Marrows, D. T. Dekadjevi, and B. J. Hickey, Phys. Rev. Lett. **85**, 4964 (2000).

[37] J. W. Freeland, V. Chakarian, K. Bussmann, Y. U. Idzerda, H. Wende, and C.-C. Kao, J. Appl. Phys. **83**, 6290 (1998).

[38] U. Ebels, M. Gester, C. Daboo, and J. A. C. Bland, Thin Solid Films **275**, 172 (1996).